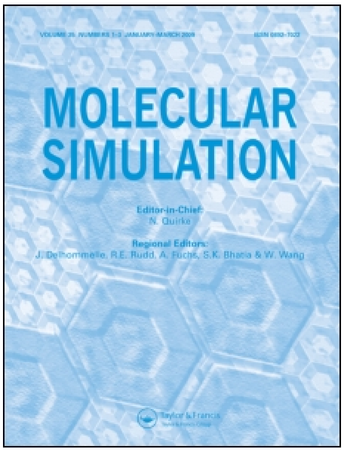

Molecular Simulation

Publication details, including instructions for authors and subscription information:
http://www.informaworld.com/smpp/title~content=t713644482

Diffusivity calculation on noble gas silica systems using first-principles molecular simulations

Liqun Zhang[ab]; Daniel J. Lacks[a]; James A. Van Orman[b]
[a] Department of Chemical Engineering, Case Western Reserve University, Cleveland, OH, USA [b] Department of Geological Sciences, Case Western Reserve University, Cleveland, OH, USA

To cite this Article Zhang, Liqun , Lacks, Daniel J. and Van Orman, James A.(2009) 'Diffusivity calculation on noble gas silica systems using first-principles molecular simulations', Molecular Simulation, 35: 10, 942 — 952

To link to this Article: DOI: 10.1080/08927020902912287

URL: http://dx.doi.org/10.1080/08927020902912287

Molecular Simulation
Vol. 35, Nos. 10–11, September 2009, 942–952

Diffusivity calculation on noble gas silica systems using first-principles molecular simulations

Liqun Zhang[ab], Daniel J. Lacks[a]* and James A. Van Orman[b1]

[a]*Department of Chemical Engineering, Case Western Reserve University, Cleveland, OH 44106, USA;* [b]*Department of Geological Sciences, Case Western Reserve University, Cleveland, OH 44106, USA*

(*Received 26 December 2008; final version received 17 March 2009*)

First-principles molecular dynamics simulations are carried out to investigate the diffusivity of noble gases dissolved in silica melts. The simulations are performed for a range of molar volumes, corresponding to pressures ranging from ambient pressure to ~50 GPa at temperatures above the SiO_2 melting point. The Chi-square merit function, weighted by the statistical certainty of the data, was used to regress the mean-square displacement against time relationship and to calculate self-diffusion coefficients for noble gases, Si, and O atoms. The results are in good agreement with the available literature data. We found that the higher the temperature and smaller the noble gas atom, the higher the diffusivity; noble gas diffusivity decreased almost linearly with the square of the atomic radius. With molar volume decreasing, the self-diffusion coefficient of small noble gases decreased, while Si and O showed an abnormal dependence on molar volume. In the temperature range simulated, the diffusivity for He, Si and O could be described by an Arrhenius equation with activation energies consistent with available experimental data within simulation accuracy.

Keywords: noble gas; diffusivity; silica melts; Einstein equation; temperature dependence

1. Introduction

Noble gases are widely used in geochemistry as tracers to gain insight into the structure of the deep Earth, its formation and differentiation, and the style and efficiency of mantle convection [1–4]. These studies depend in part on understanding the solubility and diffusivity of noble gases in silicate melts and minerals under different temperatures and pressures. The diffusion of noble gas atoms in particular are poorly known, especially at high temperature and pressure conditions as in the Earth's mantle. Experimental work on diffusion of noble gases in silicate glasses and melts is sparse [5–8]. Molecular simulations can provide essential insight into understanding noble gas diffusivity and diffusion mechanisms [9].

Previous molecular simulation studies have focused on the diffusion of small molecules in polymer materials because of its important implications for many technological applications. Besides the experimental work performed on these systems [10], molecular dynamics simulations have been used to analyse penetrant diffusion in different plastic or rubbery polymers [11–14]. Different methods to calculate diffusion coefficients in these systems have been proposed and compared [15]. The factors influencing penetrant diffusion behaviours have been investigated by [16–18]. Since silica melts and glasses have similar cage-like network structure to polymers, the results and theories could have useful implications for noble gas diffusion in liquid silica.

As a continuation of a former project [19], the same molecular simulation method based on the VASP program is used here. Previous molecular dynamics simulation methods based on empirical force fields suffer from the paucity of data to constrain the interactions of noble gas atoms with the other atoms in the system. To circumvent this issue, we have performed a study of noble gases in liquid silica using a first-principles molecular dynamics method. The simulations use non-empirical potentials based on density functional theory, and thus are not subject to the issues involved in fitting empirical potentials. But the first-principles molecular simulation approach has the limitation that it is good at working on small system with small time scale compared with empirical simulation methods, since it is computationally expensive. With both the advantage and the limitation of first-principles simulations, we investigated the noble gas diffusion behaviour in silica liquid. The method is applicable to any silicate liquid, but we chose to begin with SiO_2 because it is the simplest silicate melt and has been widely studied using other methods. Based on the simulation results, we are able to calculate the self-diffusion coefficients for Si, O, He, Ne, Ar, Kr and Xe at high temperatures and pressures without bias, and investigate the dependence of diffusivity on pressure and temperature for small noble gases.

2. Simulation details

Ab initio quantum-mechanical molecular dynamics simulations (VASP program [20–24]) were performed to study

---

*Corresponding author. Email: daniel.lacks@case.edu

ISSN 0892-7022 print/ISSN 1029-0435 online

DOI: 10.1080/08927020902912287
http://www.informaworld.com

systems containing one noble gas atom (He, Ne, Ar, Kr and Xe) and 32 SiO_2 molecules. Only one noble gas atom was included in each simulation, since noble gas solubility and concentration in silica melts are very low [5]. Ultra-soft Vanderbilt pseudopotentials (US-PP) [25,26] have been used for Si, O, Ne, Kr and Xe atoms while projector-augmented wave (PAW) pseudopotentials [27,28] were used for He and Ar atoms because of source limitation. The local density approximation (LDA) functional [29] was applied, with a plane wave cut-off of 400 eV and gamma point sampling.

VASP molecular dynamics simulations in the canonical ensemble were used, which means the system volume (V), the number of atoms in the system (N), and temperature (T) were kept constant. In order to remove surface effects, periodic boundary conditions were used. A time step of 1 fs was applied in the simulation with the interatomic forces and stresses computed at each time step and atom positions output every time step. In order to analyse the noble gas diffusivity relationship with temperature, two different temperatures were chosen: 5000 and 4000 K for each noble gas silica system. For the He system, additional simulations were performed at 3000 K. In order to observe the pressure influence on the simulation results, six molar volume ratios were used: $V/V_x = 1.0$, 0.95, 0.80, 0.70, 0.60 and 0.50 at 4000 K; $V/V_x = 1.0$, 0.95 were used at 5000 K and also at 3000 K for He; $V/V_x = 0.8$ for Ne at 5000 K. The reference volume, $V_x = 45.80\ \text{Å}^3/SiO_2$, was chosen to be the same as in Karki et al. [30] and Stixrude and Karki [31].

Simulations were performed targeting pressures from 0 to 50 GPa and the Pulay corrections were determined by continuing the simulation from an equilibrated configuration for one step using a plane cut-off of 800 eV and calculating the external pressure difference using different cut-off values. The Pulay stress correction was found to change with system size, composition, and temperature. Omitting the influences from composition and temperature, the adjusting parameter from Pulay stress is: 2.39 GPa at $V/V_x = 1.0$; 2.64 GPa at $V/V_x = 0.95$; 3.154 GPa at $V/V_x = 0.80$; 3.13 GPa at $V/V_x = 0.70$; 3.82 GPa at $V/V_x = 0.60$; and 4.78 GPa at $V/V_x = 0.50$.

In the simulation, we used both kinds of pseudopotentials (US-PP and PAW) as expressed above. In order to test whether different pseudopotentials produced equivalent results, we calculated the diffusivity using both pseudopotentials for both Ne and Xe systems at 5000 K and $V/V_x = 1.0$. Satisfactory agreement between results using different pseudopotentials was reached for both systems.

In this project, we studied the diffusivity of noble gas, Si and O atoms, and calculated self-diffusion coefficients at different temperatures and pressures. Results were compared with available literature data. The diffusion coefficients' dependence on temperature, pressure, and noble gas size was investigated.

3. Simulation results

3.1 Relationship between molar volume and pressure

We calculated pressures at different molar volumes at 4000 K for silica liquids containing five different noble gases. Neglecting the small difference in pressure from systems containing different noble gas, we averaged the pressure results from each system at the same molar volume. Regressing the results with a fourth-order polynomial, we have the results shown in Figure 1. At the smallest molar volume ($V/V_x = 0.5$), the pressure is around 46 GPa while the largest molar volume ($V/V_x = 1.0$) corresponds to a pressure around −4.5 GPa, although V_x was chosen to represent the volume of the liquid at 0 GPa (ambient pressure). This discrepancy may be ascribed to the LDA, which has a tendency of overbinding. After adjusting to the expected volume at ambient pressure, the pressures we simulated were in the range from 0 to around 50 GPa.

3.2 Noble gas diffusion in silica melts

3.2.1 Silica melts structure

Silica melts are well known for forming polymer-like network structures even at temperatures above the melting point [32,33]. At ambient pressure and 4000 K, a snapshot of the He silica system obtained using the VMD program [34,35] is shown in Figure 2. The ball located in the centre represents He, which is surrounded by a cage formed by Si—O bonds. Merging neighbouring tetrahedra formed by SiO_2 units, the cage-like structure is typical of the matrix studied by Netz and Dorfmüller [17], in which a small penetrant diffused. Compared with the rigid polymer matrix, the silica system has more flexibility since the temperatures we focused on are much higher than the SiO_2 melting point. Because of the similarity in matrix structure, we employ the same method used by [17,36,37] to analyse the diffusion trajectory with time.

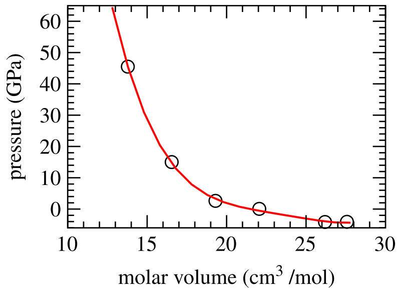

Figure 1. Molar volume and pressure relationship for liquid silica noble gas systems at 4000 K. Circles represent the simulation results, while the solid line is a fourth-order polynomial fit to the results.

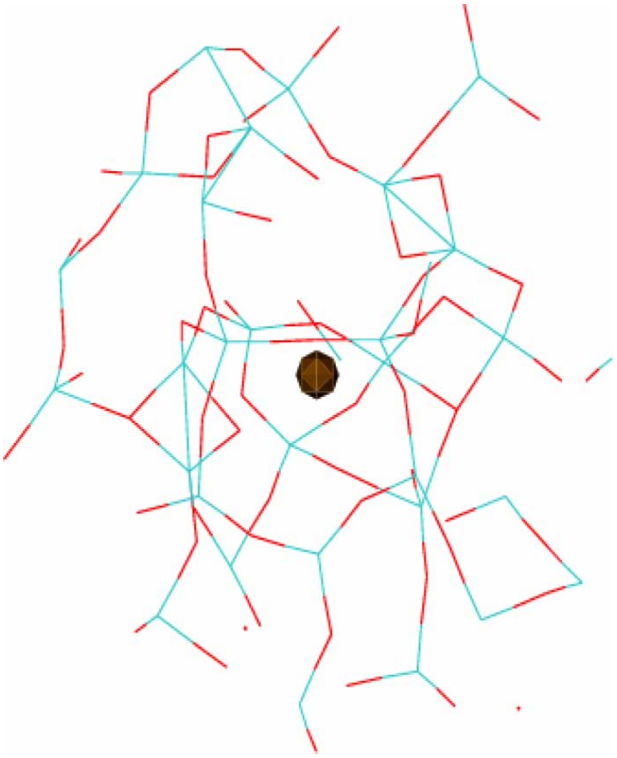

Figure 2. He in network structure of SiO_2 at 4000 K and ambient pressure. The ball represents He, while lines formed by Si and O atoms.

3.2.2 *Diffusion trajectory comparison*

He is the smallest gas atom in nature, and its diffusion trajectory along with those of Ne, Si and O, at 5000 K and molar volume ratio of 0.95 were studied first. Based on atom position results from the simulation, the mean-square displacement (MSD) of centre of mass was calculated, which has a relationship with time as:

$$\left\langle |r(t) - r(0)|^2 \right\rangle \sim t^n. \tag{1}$$

Here, r is the centre of mass position, t is the time, $\langle \cdots \rangle$ refers to the ensemble average over all times, and n is the diffusion exponent. Analysing the MSD of He with time, we observed three different stages as shown in Figure 3.

In the initially very short time, He in silica melt experiences a free flight stage (or ballistic stage), characterized by a second-order relationship between MSD and time: $\langle |r(t) - r(0)|^2 \rangle \sim t^2$.

After that, the atom experiences an anomalous stage, with the diffusion exponent smaller than 1 and larger than 0.

In the third stage, the diffusion of He obeys the Einstein equation:

$$\left\langle |r(t) - r(0)|^2 \right\rangle = 2dDt. \tag{2}$$

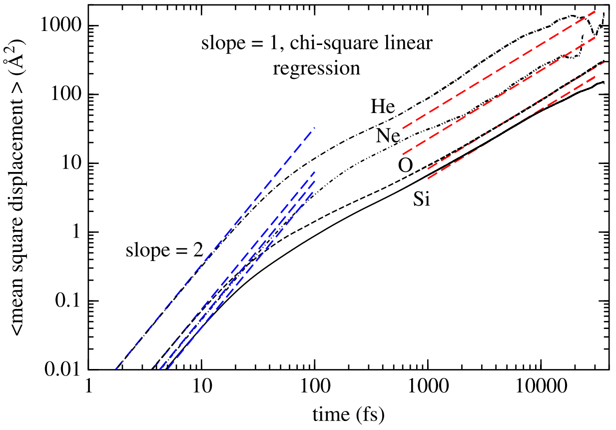

Figure 3. He, Ne, Si and O diffusion in silica melts at 5000 K and $V/V_x = 0.95$ experienced three stages: free flight stage (or ballistic stage), anomalous stage, and normal diffusion stage (or Fickian diffusion stage). The slope = 1 fit comes from Chi-square linear regression weighted by the statistical certainty of the data, as discussed in a later section.

Here, D is the diffusion coefficient, and d is the dimensionality, which equals 3 in our system. During this normal diffusion stage, the MSD has a linear relationship with time. Similarly, for Ne, Si and O at 5000 K and $V/V_x = 0.95$, their MSD and time plots also showed three stages: free-flight stage, anomalous stage, and normal diffusion stage. Comparing the tail part on the plots, we could see that Si and O kept their normal diffusion till the end, while noble gases have fluctuations arising from numerical noise. The noise is much greater for the noble gas atoms than for Si and O because there is only one noble gas atom in each simulation, while there are 32 Si atoms and 64 O atoms.

3.2.3 *Diffusion exponent calculation*

The time of the transition from anomalous diffusion to normal diffusion is defined as the crossover time, while the corresponding accumulated displacement is defined as the crossover distance [16]. Since diffusion stages are characterized by typical diffusion exponent values, the crossover time and crossover distance could be determined using a revised form of Equation (1) as follows:

$$\ln\left(\left\langle |r(t) - r(0)|^2 \right\rangle\right) = n \ln t + \text{constant}. \tag{3}$$

Calculating the differentiation of $\ln(\langle |r(t) - r(0)|^2 \rangle)$ over $\ln(t)$ in consecutive times with a time step of 1 fs, we have the diffusion exponent results for He, Ne, Si and O at 5000 K and $V/V_x = 0.95$ shown in Figure 4.

Based on Cuthbert et al. [15], the normal (or Fickian) diffusion regime could be decided to be the time interval during which the diffusion exponent remained within 10%

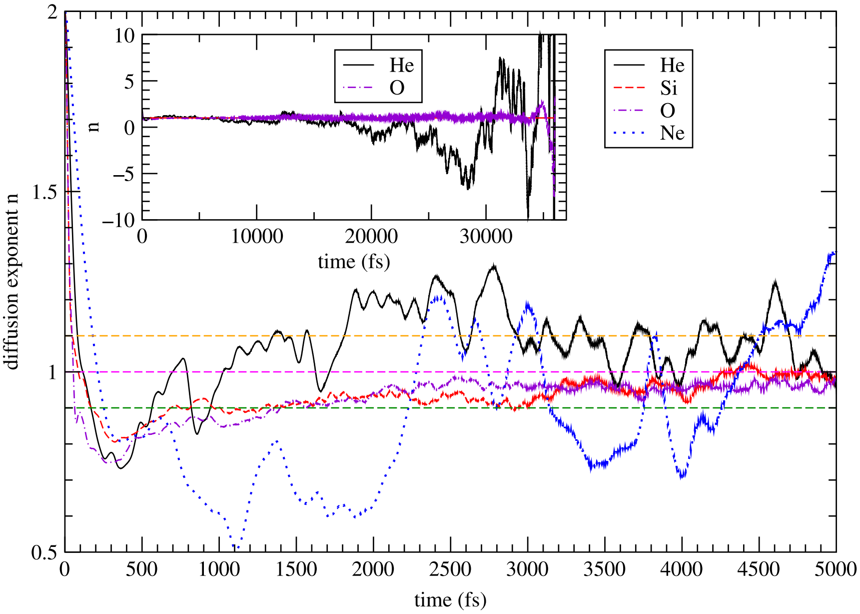

Figure 4. Diffusion exponents with time in silica melts at 5000 K and $V/V_x = 0.95$ for: He (solid line), Ne (dashed line), Si (dot dashed line) and O (dotted line), with the He and O diffusion exponents also shown in the inset.

of 1.00. Using that rule, reference lines at 1.1, 1.0, and 0.9 are shown in Figure 4 to show the regime of normal diffusion behaviour. The He diffusion exponent dropped from an initial value of 2 to a valley of 0.73 rapidly, then increased to a value around 1 in several hundred femtoseconds. After that, it fluctuated around the reference lines for around 22 ps as shown in the inset of Figure 4, until its fluctuation increased to a much larger range, synchronized with the large fluctuations in the tail shown in Figure 3. The Ne diffusion exponent fluctuated in a larger range compared with that of He and increased to the normal diffusion reference lines after several picoseconds. Both He and Ne have much more noise than Si and O, which increased rapidly to an exponent of 0.9 at around 1.4 ps, then kept on consistently within the reference lines until the very end, with exponent of O over the whole range shown in the inset of Figure 4. Based on the crossover time of Si and O, a crossover distance of 10 Å^2 was determined from Figure 3.

Comparing the diffusion exponent results from He and Ne, we found that the smaller the noble gas size, the shorter the crossover time. The large deviation of diffusion exponents from reference values for noble gases at long times is consistent with the large fluctuations on the MSD versus time plots.

3.2.4 *Chi-square merit function linear regression*

For noble gases, large fluctuations at the tail of the MSD over time curve and diffusion exponent over time results, in a range up to half of the simulation time as shown in Figures 3 and 4, caused ambiguity in deciding the normal diffusion range and calculating the diffusion coefficient using the Einstein equation.

We calculated the centre of mass displacements based on all possible starting times, and obtained averages of the MSD as a function of time interval t. Based on that, for a simulation time of N fs with atom position output every femtosecond, at time 1, there are $N-1$ data points for the MSD calculation, and at time t, there are only $N-t$ data points being used to calculate the average. At the last point, time N, there is only one data point on the MSD against time curve. So, with time increasing, the numerical noise increases because fewer data are available. In order to estimate the slope from the figure with certainty and also to take into account the uncertainties at the tail, we used a numerical Chi-square minimization method to estimate the slope. We estimate the uncertainty σ associated with each time as follows:

$$\sigma = 1/\sqrt{(N-t)}. \tag{4}$$

Based on Press et al. [38], in order to linearly regress the MSD against time curve including uncertainties, we used the Chi-square merit function to measure how well the equation agrees with the data, as follows:

$$\chi^2(a,b) = \sum_{t=0}^{N} \left(\frac{\left\langle |r(t) - r(0)|^2 \right\rangle - 2dDt}{\sigma} \right)^2. \tag{5}$$

Here, $2dD$ is the slope. Using solver tool in excel software, we get the best estimation for 6D at the minimum of χ^2, with linear fitting as shown in Figure 3. The linear fitting line for Si, O, and Ne almost overlapped the original line in the normal diffusion regime, while the best fit line is lower than the original line for He after balancing the huge drop at its tail.

3.2.5 *Larger noble gases diffusion behaviour*

For larger noble gases (Ar, Kr and Xe), we could observe a trustable normal diffusion range only at the high temperature and the lowest pressure on the MSD over time plots, with simulation results and Chi-square merit function linear regression results shown in Figures 5 and 6. In Figure 5, the linear fitting lines and the original lines are very close and consistent with each other in the normal diffusion regime, while those two have larger gaps in Figure 6 since the MSD over time curves fluctuated more. Comparing the diffusivities among the five noble gases, He diffused much faster than Ne, which diffused much faster than the large noble gases. During the simulation time, we observed that Xe diffused the slowest, and Kr diffused slower than Ar (although at short times it appeared to be faster). At 4000 K, Ar showed a tendency to diffuse much faster than Kr as shown in Figure 6. Insufficient simulation time and poor statistics explain the occasional faster diffusion of Kr, and also the larger gaps between the regression line and the original curve in the normal diffusion regime on the noble gas MSD over time curves at 4000 K.

3.2.6 *Diffusion results*

Based on parameter estimation results from Chi-square merit function weighted by statistical certainty of the data, we calculated the diffusion coefficient of noble gases at 4000, 5000 K, and ambient pressure, with results shown in Table 1. Averaging the four longest simulation results we performed over consecutive time interval of 4 ps, we calculated the standard deviation (SD) for the diffusion coefficients, with a value up to 20% for He and Ne, and up to 40% for larger noble gases. Using the same method, we calculated the Si and O diffusion coefficients at different temperatures and pressures. Averaging the results from all five systems (containing each of the noble gases), we calculated the average diffusion coefficients and SDs for Si and O, which are also shown in Table 1.

Based on the self-diffusion coefficient results, we found that with noble gas size increasing from He to Xe, the noble gas diffusion coefficient decreased. Small noble gases diffused much faster than O atoms, which diffused slightly faster than Si atoms. With temperature increasing, the diffusion rate of all atom types increased.

Comparing our diffusion coefficient results for Si and O at both 4000 and 5000 K, and $V/V_x = 1.0$ with those from Karki et al. [30], a satisfactory agreement was found. Guissani and Guillot [36] calculated the diffusion coefficients of He, Ne, Ar and Kr in silica melts at 4000 and 6000 K and ambient pressure using empirical molecular dynamics simulations. Comparing the self-diffusion coefficient of noble gases, Si, and O with ours led

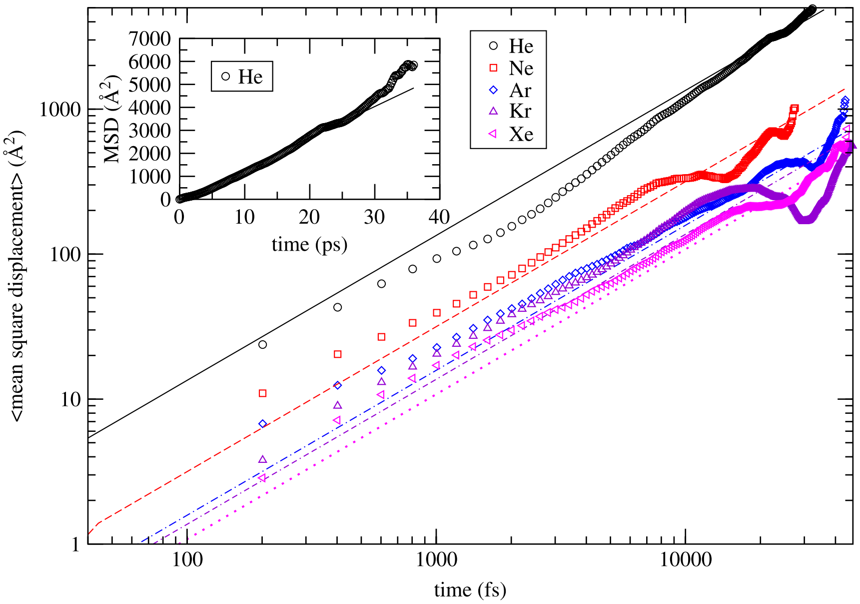

Figure 5. MSD against time for five kinds of noble gases: He (open circle) with its whole trajectory also shown in the inset, Ne (open square), Ar (open diamond), Kr (upside triangle), and Xe (left-side triangle) diffusion at 5000 K and $V/V_x = 1.0$, with lines from linear regression with Chi-square merit function weighted by the statistical certainty of the data: He (solid line), Ne (dashed line), Ar (dash-dot-dashed line), Kr (dot-dashed line) and Xe (dotted line).

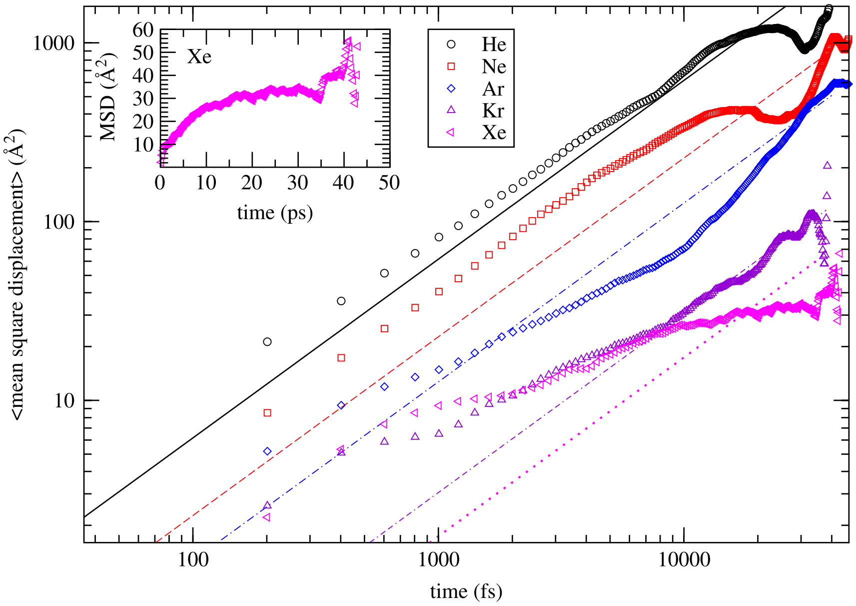

Figure 6. MSD against time for five kinds of noble gases: He (open circle), Ne (open square), Ar (open diamond), Kr (upside triangle), and Xe (left-side triangle) with its whole trajectory also shown in the inset at 4000 K and $V/V_x = 1.0$, with lines from linear regression with Chi-square merit function weighted by the statistical certainty of the data: He (solid line), Ne (dashed line), Ar (dash-dot-dashed line), Kr (dot-dashed line) and Xe (dotted line).

Table 1. Diffusion coefficients results of Si, O, and noble gases at 4000 and 5000 K, and ambient pressure.

Temperature (K)	D_{Si} ($\times 10^{-5}$ cm^2/s)	D_O ($\times 10^{-5}$ cm^2/s)	D_{He} ($\times 10^{-5}$ cm^2/s)	D_{Ne} ($\times 10^{-5}$ cm^2/s)	D_{Ar} ($\times 10^{-5}$ cm^2/s)	D_{Kr} ($\times 10^{-5}$ cm^2/s)	D_{Xe} ($\times 10^{-5}$ cm^2/s)
4000	2.1 ± 0.9	2.7 ± 0.8	103 ± 5	38 ± 7	21 ± 4	5 ± 2.1	3 ± 1.2
5000	12.8 ± 1.7	14.1 ± 1.2	224 ± 29	63 ± 11	26 ± 6	22 ± 10	18 ± 5

to consistently smaller values by around 50% at 4000 K from Guissani and Guillot [36].

3.3 *Tests of reproducibility*

In the simulations, we have only one noble gas atom in each system. Poor statistics result in noisy simulation results as expected. In order to make sure the simulation results are trustable, besides running long time simulation (around 50 ps in VASP) and using both kinds of pseudopotentials to run simulations for Ne and Xe at 5000 K and ambient pressure, we reran simulations from different initial configurations. For Ne in silica system at 5000 K, we initially equilibrated the system using NPT ensemble for 4 ps. After the volume of the system reached the reference volume at ambient pressure, we continued the simulation with NVT for at least 28 ps. Calculating the diffusion coefficients from the rerun simulation, a diffusion coefficient around 58×10^{-5} cm^2/s, with a deviation of 12×10^{-5} cm^2/s was reached, consistent with the original simulation result of 63×10^{-5} cm^2/s with a deviation of 11×10^{-5} cm^2/s.

We also performed a simulation on a system with higher noble gas concentration: 4 He atoms and 32 SiO2 at 5000 K and ambient pressure. After running the simulation for 5 ps, we calibrated the diffusion coefficients of three atom types with the MSD results shown in Figure 7. The diffusion

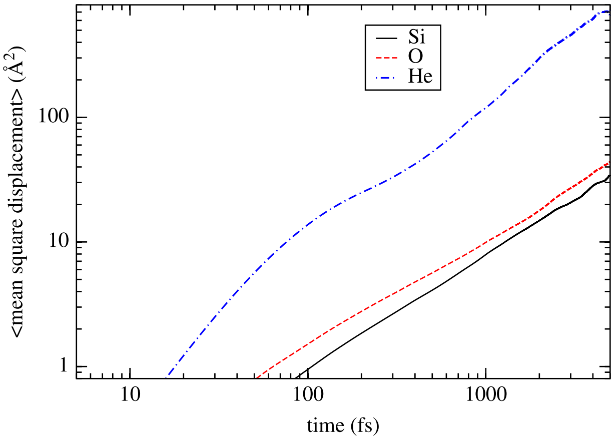

Figure 7. MSD against time for Si (solid line), O (dashed line), and He (dash-dot-dashed line) in 4 He and 32 SiO_2 melt at 5000 K and ambient pressure.

coefficient is 263.6 × 10^{-5} cm^2/s for He, 11 × 10^{-5} cm^2/s for Si, and 14.3 × 10^{-5} cm^2/s for O. These results are in good agreement with the original result for the system with one He atom.

3.4 Diffusivity dependence on temperature

Murphy et al. [39] estimated the cage residency time (which correlates to the energy barrier small atom need to overcome in diffusion) for He, Ne and Ar at room temperature (300 K) in the silicate mineral sodalite using transition state theory. The cage residency time for He is only 23 ps, while for Ne it is 140 ns and for Ar it could not be calculated due to being trapped on the laboratory time scale. Since we worked at much higher temperatures (at least 10 times higher), the cage residency time and diffusion relaxation time for small molecules should be much shorter. Based on the molecule size, temperature and relaxation time relationship found by Zhang and Greenfield [40], with the noble gas size increasing and temperature decreasing, the diffusion relaxation time should increase rapidly. Thus, much longer simulation time is required to calculate diffusion coefficients for larger noble gases reliably, especially at low temperature (3000 K). Because VASP simulations are very expensive, we only calculated He diffusion at the lowest temperature at $V/V_x = 0.95$ in this project, and analysed its diffusivity–temperature relationship, along with Si and O, with results shown in Figure 8. With temperature decreasing, the diffusion rate of He, Si, and O decreased. The diffusion and temperature relationship could be described well using the Arrhenius equation,

$$\log(D(T)) = \log(D_0) - \frac{E_a}{RT}. \qquad (6)$$

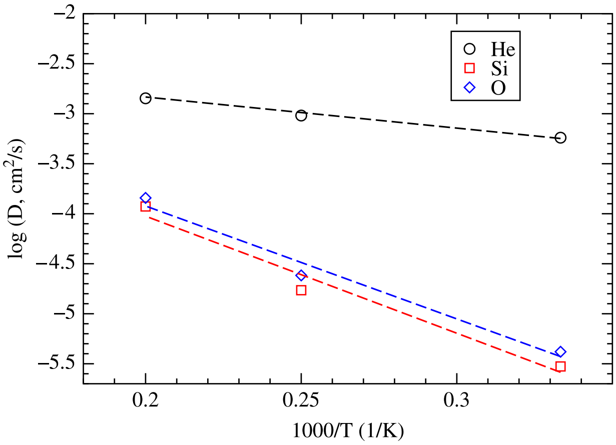

Figure 8. He, Si, and O diffusion coefficients relationship with temperature at $V/V_x = 0.95$.

Here, R is the gas constant, D_0 is the pre-exponential parameter, T is the temperature, and E_a is the activation energy.

Based on the regression results, we calculated the He diffusion activation energy as 59.5 kJ/mol with a deviation of 11 kJ/mol. Carroll et al. [41] analysed noble gas diffusion in silica glass from 700 to 950 centigrade and 215 to 3150 bar, and calculated an activation energy of 27.6 kJ/mol. Abe et al. [6] analysed noble gas diffusion in fused silica using both isothermal and non-isothermal measurements in a temperature range of 523 to 763 centigrade. They obtained an activation energy of 26.8 to 29.7 kJ/mol. Comparing with experimental data, our activation energy was doubled. Since we calculated the He diffusion coefficients at much higher temperatures, thus in a more mobile matrix, such a deviation is not surprising. Because of the large difference between glass and liquid diffusion activation results, it is not reasonable to extrapolate diffusion coefficient results from the high temperature range (liquid state) to the low temperature range (glass state) since the dynamics of the matrix is very important to the diffusion threshold [16].

We also estimated the activation energies for Si and O in a temperature range of 3000–5000 K at $V/V_x = 0.95$, with an activation energy of 221.8 kJ/mol and a deviation around 42 kJ/mol for both Si and O. Compared with He, diffusion of Si and O have a much stronger temperature dependence in the same temperature range. Litton and Garofalini [42] calculated the activation energy for Si and O in the temperature range of 4800–7200 K, with a result of 481.2 and 477 kJ/mol for Si and O individually. Our results could only reach around 1/2 of theirs. Karki et al. [30] calculated the diffusion activation energy for both Si and O as 309.6 kJ/mol at a temperature range of 2500–6667 K at ambient pressure using first-principles molecular simulations. Their results are slightly higher than ours. Since we worked on a smaller temperature range and had fewer data, a difference of such magnitude is not surprising.

3.5 Diffusivity dependence on pressure

Besides temperature, we analysed the influence of pressure on the diffusion rate of He, Ne, Si and O atoms in silica melts.

3.5.1 Noble gas diffusion coefficients at different pressures

With molar volume decreasing (pressure increasing), the diffusion rates of small noble gas atoms decreased. Using Ne as an example with results shown in Figure 9, as the molar volume ratio decreased from 1.0 to 0.80, the slope of the MSD versus time curve decreased. The Chi-square linear fitting weighted by statistical certainties of the data

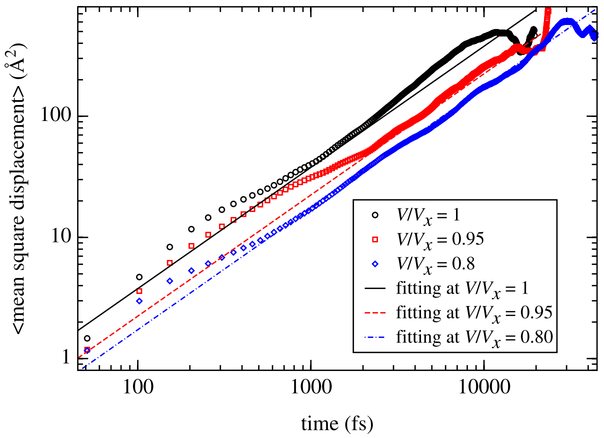

Figure 9. Diffusion for Ne at $V/V_x = 1.0$ (open circles), $V/V_x = 0.95$ (open square), and $V/V_x = 0.80$ (open diamond) at 5000 K, with lines from Chi-square merit fitting weighted by the statistical certainty of the data, for volume ratio equals 1.0 (solid line), 0.95 (dashed line), 0.80 (dot dashed line).

also agreed well with the original curve in the normal diffusion regime at short times. Analysing the relationship between diffusivity and molar volume for the two smallest noble gases, we have results shown in Figure 10(a). With molar volume decreasing (pressure increasing), the diffusion coefficients for both He and Ne decreased: the higher the pressure, the slower the noble gas diffusion rate; and He always diffused faster than Ne because of its smaller size. Based on the relationship between molar volume and pressure, we calculated the activation volume for noble gases with a result of 2.2 cm^3/mol for He at 4000 K. Ne has a similar activation volume, but it is much less well constrained due to the greater uncertainty in the diffusion results. The activation volume for both minerals appears to decrease significantly at pressures beyond 20 GPa, as expected due to the significantly lesser compressibility of the melt at such high pressures.

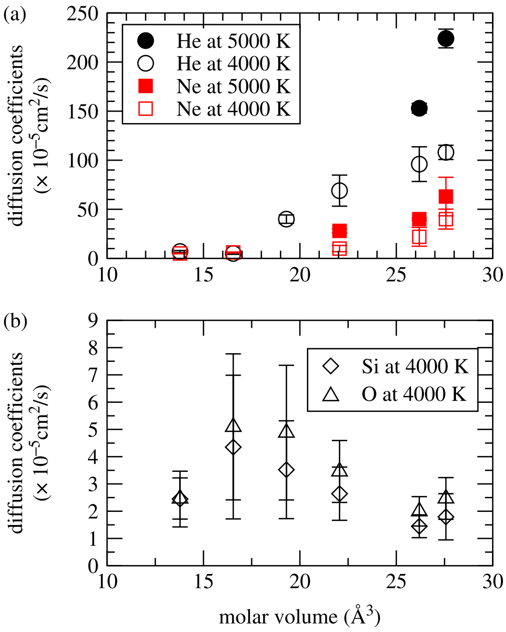

Figure 10. Diffusion coefficients at different molar volumes for He (open circles) and Ne (open squares) at 4000 and 5000 K; for Si (open diamond) and O (open triangle) at 4000 K.

3.5.2 Si and O diffusion coefficients relationship with pressure

Analysing Si and O average diffusion coefficients at different molar volumes at 4000 K, we have the results shown in Figure 10(b). With molar volume ratio decreasing from 1.0 to 0.6, the diffusion coefficients for both Si and O increased, then decreased up to $V/V_x = 0.50$. Comparing the diffusion results with Karki et al. [30], we found a good agreement with their data on both absolute diffusion results and their (molar volume) pressure dependence within the simulation accuracy. The anomalous Si and O diffusivity dependence on molar volume was consistent with what Angell et al. [43] found, who attributed the prevalence of fivefold coordination of silica ions to the diffusivity maximum occurring at the pressure of 20–30 GPa. Shimizu and Kushiro [32] confirmed the oxygen anomalous diffusivity dependence on pressure in silicate melts using experiments, and analysed the structure relationship with transport properties for two kinds of silicate melts (jadeite and diopside). In the molar volume ratio range of 0.95 to 0.6, we observed almost linear Si and O diffusivity dependence on molar volume, with the diffusivity for both Si and O increased by a factor of 3, which is a little larger than that Shimizu and Kushiro found (a factor of 2), but close to what Angell et al. found in the pressure range from 1 atm to 20 GPa. We observed the initial drop in Si and O diffusivity on molar volume ratio from 1 to 0.95 as Karki did [30] (from 1 to 0.90), which could be ascribed to the simulation noise.

Comparing the diffusion coefficient dependence on pressure (molar volume) among atoms in the system, solvent atoms Si and O diffused faster at higher pressures as the silicate network collapses; while solute atoms He and Ne diffusion rate decreased with pressure increasing, appearing to be insensitive to changes in the network structure.

3.6 Noble gases diffusivity relationship with square of radii

Lux [8] have investigated the solubility and diffusivity of light gases in silicate liquids and found that both the solubility and diffusion coefficients (on a logarithmic scale) could relate almost linearly with the square of noble gas radius. Based on the diffusion coefficient results at $V/V_x = 1.0$ for He, Ne, Ar, Kr and Xe, diffusivity

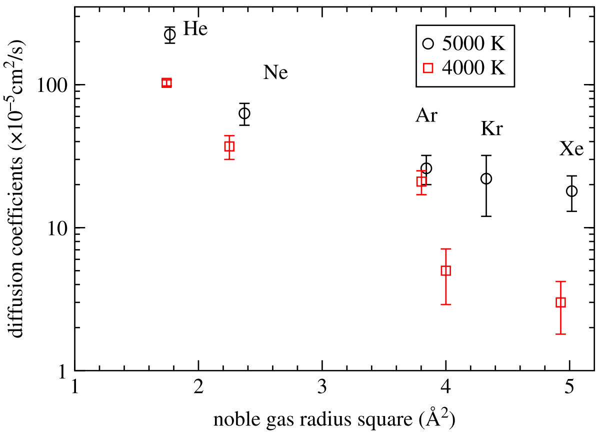

Figure 11. Noble gas diffusion coefficients relationship with square of radii at 5000 K (open circle) and 4000 K (open diamond) at $V/V_x = 1.0$.

relationship with the square of radii were analysed at 4000 and 5000 K, with results shown in Figure 11. Using the same method as described in a former publication [19], we estimated the equilibrium atomic radii for the five different noble gases. Figure 11 showed that at both 4000 and 5000 K, the diffusion coefficients of noble gases have an almost linear relationship with the square of radii. Comparing those results with data at 1350 centigrade and ambient pressure from Lux [8], a similar tendency between diffusion coefficients and square of radii for He and Ne was found.

With noble gas size increasing from He to Xe, the diffusion coefficients decreased. At 4000 K, the diffusion coefficient of He is around 34 times larger than that of Xe, while at 5000 K, there is only a factor around 13 between those two. Such kind of diffusion coefficient ratio was very close to findings from Lux (a factor around 20), although the absolute diffusion coefficients of noble gases from ours were much larger.

4. Discussion

Based on the simulation time we performed, only the small noble gases He and Ne could be examined in terms of the relationship of diffusivity with temperature and pressure. Larger noble gases like Ar, Kr and Xe have longer diffusion relaxation time and we observed anomalous diffusion during the simulation time except at the high-temperature and low-pressure conditions. Such results are consistent with conclusions from Nets and Dorfmüller [17], who analysed the diffusion of solutes in cage-like structures (like silica melt network) and found that a pronounced anomalous diffusion would prevail with the tracer radius larger than 80% of the mean pore radius. Since noble gases diffused in silica melts by ion migrations, the non-overlapping interstice size in the system could influence their transport behaviour. Malavasi et al. [44] using Voronoi–Delaunay approach calculated the void size distribution in silica glasses with non-overlapping interstice sizes (pore radius) distributed in a range of no more than 2.18 Å. Comparing the interstice size with the radii of He, Ne, Ar, Kr and Xe at ambient pressure, which are 1.32, 1.50, 1.96, 2.01 and 2.19 Å respectively at 4000 K, we found that the noble gases were inside the pore radius range except Xe. Since we work on silica melts at high temperatures, the pore size in our simulation condition should be larger than that Malavasi et al. found. So the noble gases have possibilities to diffuse freely in the pore if their radii are no more than 80% of the pore radius. With pressure increasing, both the noble gas radii and the pore radius decrease, and the obstacle from the silica matrix increases rapidly, so we could only observe small noble gases (He and Ne) diffusing freely without being trapped at low pressures in the simulation time we performed.

In the simulation, we found the noble gas diffusion rates decreased with molar volume decreasing, while the diffusion of Si and O atoms showed a nonlinear relationship with molar volume (pressure). With molar volume decreasing, the diffusion of Si and O atoms increased to the maximum at $V/V_x = 0.60$, then decreased up to $V/V_x = 0.50$. Such kind of anomalous diffusivity dependence on pressure demonstrated that both Si and O diffused by the collapse of network, while noble gases (He and Ne) diffusivity behaviour on pressure showed an ion migration mechanism [32].

Müller-Plathe et al. [11] investigated the diffusion of He and O_2 molecules in amorphous polymers and found that the MSD of He atoms in polyisobutylene in the supposed normal diffusion range still had certain amount of anomalous diffusion although the diffusion coefficient calculated in that range agreed with experimental data well. The diffusion of penetrant in rigid or amorphous matrix could be very complex. In our noble gas silica melt simulations, it is not surprising to find that it could be very difficult to define an exact normal diffusion range based on the MSD against time relationship. In order to calculate the diffusion coefficients for noble gases in silica melts satisfactorily, a much longer simulation time (for example, several nanoseconds) could be required. Since VASP simulation is very expensive, we need to balance accuracy and expense, and the diffusion coefficient was estimated by Chi-square merit function fitting weighted by the statistical certainty of the data. By comparing our results with literature data, the present noble gas diffusion results could capture the essence of penetrant motion in silica melts, and present us with reasonable results.

5. Conclusions

From the present first-principles molecular dynamics simulation study of the diffusion of five different noble gases in silica melts, the following conclusions can be made: (1) the larger the noble gas size, the smaller the diffusion coefficient; (2) Arrhenius-type behaviour with temperature was observed, with activation energy of 59.5, 221.8, and 221.8 kJ/mol for He, Si and O, respectively; and (3) with molar volume ratio decreasing from 1 to 0.6, the diffusion coefficients of Si and O increased, while the diffusion coefficients for He and Ne decreased.

Another important conclusion is that, for small molecule diffusion in flexible matrix like liquid silica, the Chi-square linear-regression model could estimate the self-diffusion coefficient semi-quantitatively based on limited first-principles simulation results. By repeating simulations from different initial configurations and using different pseudopotentials, and comparing results with system having better statistics on noble gas, the present diffusion results are reliable within simulation accuracy.

Acknowledgements

This work was supported through grants from the National Science Foundation (NSF). Thanks to the Ohio Supercomputer Center, which provided supercomputing resources for the VASP simulations.

Note

1. Email: james.vanorman@case.edu

References

[1] C.J. Allégre, T. Staudacher, and P. Sarda, *Rare gas systematics: formation of the atmosphere, evolution and structure of the Earth's mantle*, Earth Planet. Sci. Lett. 81 (1987), pp. 127–150.

[2] C.J. Allégre, A. Hofmann, and K. O'Nions, *The argon constraints on mantle structure*, Geophys. Res. Lett. 23 (1996), pp. 3555–3557.

[3] M. Ozima and G.T. Igarashi, *The primordial noble gases in the Earth: a key constraint on Earth evolution models*, Earth Planet. Sci. Lett. 176 (2000), pp. 219–232.

[4] S.W. Parman, *Helium isotopic evidence for episodic mantle melting and crustal growth*, Nature 446 (2007), pp. 900–903.

[5] M.R. Carroll and E.M. Stolper, *Noble gas solubilities in silicate melts and glasses: new experimental results for argon and the relationship between solubility and ionic porosity*, Geochim. Cosmochim. Acta 57 (1993), pp. 5039–5051.

[6] M. Abe, B. Rauch, and W.W. Brandt, *Nonisothermal diffusion measurements on granular solids: noble gas diffusion in fused silica*, Z. Naturforsch. Teil A 26 (1971), pp. 997–1004.

[7] J.E. Shelby, *Solubility and diffusion of inert gases in silicate melts*, in *18th International Congress on Glass*, San Francisco, CA, 1998.

[8] G. Lux, *The behavior of noble gases in silicate liquids: solution, diffusion, bubbles and surface effects, with applications to natural samples*, Geochim. Cosmochim. Acta 51 (1987), pp. 1549–1560.

[9] D.I. Kopelevich and H. Chang, *Diffusion of inert gases in silica sodalite: importance of lattice flexibility*, J. Chem. Phys. 115 (2001), pp. 9519–9527.

[10] M.T. Cicerone, F.R. Blackburn, and M.D. Ediger, *Anomalous diffusion of probe molecules in polystyrene: evidence for spatially heterogeneous segment dynamics*, Macromolecules 28 (1995), pp. 8224–8232.

[11] F. Müller-Plathe, S.C. Rogers, and W.F. van Gunsteren, *Computational evidence for anomalous diffusion of small molecules in amorphous polymers*, Chem. Phys. Lett. 199 (1992), pp. 237–243.

[12] A.A. Gusev, S. Arizzi, U.W. Suter, and D.J. Moll, *Dynamics of light gases in rigid matrices of dense polymers*, J. Chem. Phys. 99 (1993), pp. 2221–2227.

[13] A.A. Gusev and U.W. Suter, *Dynamics of small molecules in dense polymers subject to thermal motion*, J. Chem. Phys. 99 (1993), pp. 2228–2234.

[14] M.L. Greenfield, *Simulation of small molecule diffusion using continuous space disordered networks*, Mol. Phys. 102 (2004), pp. 421–430.

[15] T.R. Cuthbert, N.J. Wagner, M.E. Paulaitis, G. Murgia, and B. D'Aguanno, *Molecular dynamics simulation of penetrant diffusion in amorphous polypropylene: diffusion mechanism and simulation size effects*, Macromolecules 32 (1999), pp. 5017–5028.

[16] H. Weber and W. Paul, *Penetrant diffusion in frozen polymer matrices: a finite-size scaling study of free volume percolation*, Phys. Rev. E 54 (1996), pp. 3999–4007.

[17] P.A. Netz and T. Dorfmüller, *Computer simulation studies of diffusion in gels: model structures*, J. Chem. Phys. 107 (1997), pp. 9221–9233.

[18] J.H.D. Boshoff, R.F. Lobo, and N.J. Wagner, *Influence of polymer motion, topology and simulation size on penetrant diffusion in amorphous, glassy polymers: diffusion of helium in polypropylene*, Macromolecules 34 (2001), pp. 6107–6116.

[19] L. Zhang, J.A. Van Orman, and D.J. Lacks, *Effective radii of noble gas atoms in silicates from first principles molecular simulation*, Am. Mineral. 94 (2008), pp. 600–608.

[20] G. Kresse and J. Furthmüller (2008), VASP home page, http://www.cms.mpi.univie.ac.at/vasp/vasp/vasp.html

[21] G. Kresse and J. Furthmüller, *Efficiency of* ab-initio *total energy calculations for metals and semiconductors using a plane-wave basis set*, Comput. Mat. Sci. 6 (1996), pp. 15–50.

[22] G. Kresse and J. Hafner, Ab initio *molecular dynamics for liquid metals*, Phys. Rev. B 47 (1993), pp. 558–561.

[23] G. Kresse and J. Hafner, Ab initio *molecular-dynamics simulation of the liquid-metal-amorphous-semiconductor transition in germanium*, Phys. Rev. B 49 (1994), pp. 14251–14269.

[24] G. Kresse and J. Furthmüller, *Efficient iterative schemes for* ab initio *total-energy calculations using a plane-wave basis set*, Phys. Rev. B 54 (1996), pp. 11169–11186.

[25] D. Vanderbilt, *Soft self-consistent pseudopotentials in a generalized eigenvalue formalism*, Phys. Rev. B 41 (1990), pp. 7892–7895.

[26] G. Kresse and J. Hafner, *Norm-conserving and ultrasoft pseudopotentials for first-row and transition-elements*, J. Phys. Condens. Matter. 6 (1994), pp. 8245–8257.

[27] G. Kresse and D. Joubert, *From ultrasoft pseudopotentials to the projector augmented-wave method*, Phys. Rev. B 59 (1999), pp. 1758–1775.

[28] P.E. Blöchl, *Projector augmented-wave method*, Phys. Rev. B 50 (1994), pp. 17953–17979.

[29] J.P. Perdew and A. Zunger, *Self-interaction correction to density-functional approximations for many-electron systems*, Phys. Rev. B 23 (1981), pp. 5048–5079.

[30] B.B. Karki, D. Bhattarai, and L. Stixrude, *First-principles simulations of liquid silica: structural and dynamical behavior at high pressure*, Phys. Rev. B 76 (2007), 104205.

[31] L. Stixrude and B. Karki, *Structure and freezing of $MgSiO_3$ liquid in Earth's lower mantle*, Science 310 (2005), pp. 297–299.

[32] N. Shimizu and I. Kushiro, *Diffusivity of oxygen in jadeite and diopside melts at high pressures*, Geochim. Cosmochim. Acta 48 (1984), pp. 1295–1303.

[33] C.M. Scarfe, B.O. Mysen, and D. Virgo, *Pressure dependence of the viscosity of silicate melts*, in *Magmatic Processes: Physicochemical Principles*, B.O. Mysen, ed., Geochemical Society, University Park, 1987, pp. 59–67.

[34] W. Humphrey, A. Dalke, and K. Schulten (2008), vmd home page, http://www.ks.uiuc.edu/Research/vmd/

[35] W. Humphrey, A. Dalke, and K. Schulten, *VMD – visual molecular dynamics*, J. Mol. Graph. 14 (1996), pp. 33–38.

[36] Y. Guissani and B. Guillot, *Transport of rare gases and molecular water in fused silica by molecular dynamics simulation*, Mol. Phys. 95 (1998), pp. 151–162.

[37] G.D. Luca, P. Pullumbi, G. Barbieri, A.D. Famá, P. Bernardo, and E. Drioli, *Gusev and Suter calculation of the diffusion coefficients of light gases in silicate-1 membrane and silica-sodalite zeolite*, Sep. Purif. Technol. 36 (2004), pp. 215–228.

[38] W.H. Press, B.P. Flannery, S.A. Teukolsky, and W.T. Vetterling, *Numerical Recipes*, Cambridge University Press, Cambridge, 1987.

[39] M.J. Murphy, G.A. Voth, and A.L.R. Bug, *Classical and quantum transition state theory for the diffusion of helium in silica sodalite*, J. Chem. Phys. 101 (1997), pp. 491–503.

[40] L. Zhang and M.L. Greenfield, *Relaxation time, diffusion, and viscosity analysis of model asphalt systems using molecular simulation*, J. Chem. Phys. 127 (2007), 194502.

[41] M.R. Carroll, S.R. Sutton, M.L. Rivers, and D.S. Woolum, *An experimental study of krypton diffusion and solubility in silicic glasses*, Chem. Geol. 109 (1993), pp. 9–28.

[42] D.A. Litton and S.H. Garofalini, *Vitreous silica bulk and surface self-diffusion analysis by molecular dynamics*, J. Non-Cryst. Solids 217 (1997), pp. 250–263.

[43] C.A. Angell, P.A. Cheeseman, and S. Tamaddon, *Pressure enhancement of ion mobilities in liquid silicates from computer simulation studies to 800 kilobars*, Science 218 (1982), pp. 885–887.

[44] G. Malavasi, M.C. Menziani, A. Pedone, and U. Segre, *Void size distribution in MD-modelled silica glass structures*, J. Non-Cryst. Solids 352 (2006), pp. 285–296.